Detection of bearing fault by scalar indicator X.

Abstract : Bearing reliability is essential in industrial systems, and their vibration monitoring remains a challenge for anticipating failures. In this work, two classic scalar indicators were considered: the root mean square (RMS) value and kurtosis. This allowed for the development of a new indicator that takes into account the number of peaks exceeding the RMS value. The results obtained on two datasets, one with four different frequencies (10, 20, 30, and 40 Hz) and the other with a single frequency of 24 Hz, are promising. The RMS and kurtosis indicators are limited in their ability to detect different types of defects. It is in this context that, in this work, we developed a new scalar indicator, X, obtained using the two indicators mentioned above. This indicator offers more reliable and robust discrimination of bearing conditions and allows not only the detection of a defect but also a better characterization of its nature. Full-scale tests will validate this new indicator for its simple use in analyzers for the analysis of stationary signals in the time domain.

Keywords :bearing; vibration analysis; predictive maintenance; X scalar indicator; time analysis.

1. Introduction

In most industrial sectors, rotating machinery forms the core of production processes.They largely perform the vital function. They enable the production of rotational movements capable of carrying out mechanical drives (crushing, pulling, extraction, etc.).They are also used in electricity production.Regardless of the field of operation, they experience failures during their use. An unexpected failure in a production rotating machine most often has serious consequences for operators because it could halt production and generate economic losses. Maintenance should therefore no longer be limited to repairs alone, but must go further by predicting and anticipating malfunctions. To achieve these objectives, several maintenance methods have been developed in recent years thanks to research and technologies for diagnosing and monitoring the degradation of machines. Among these methods, vibration analysis has become a benchmark in the detection and diagnosis of rotating machinery (Djebili, 2013; Mounia, 2018; Hotait, 2020).Bearings, as transmission components, play a crucial role in ensuring continuous operation. Their progressive degradation is one of the main causes of unplanned downtime, leading to high maintenance and production costs. Statistical studies conducted in 2008 by Bonnet on high-power asynchronous machines used in industry showed that 69% of failures were located in the bearings. This percentage was 41% in 2001 (*Figure 1*). Indeed, bearings play a central role in transmitting loads and reducing friction. In this context, the early diagnosis of bearing failures is a major challenge for the reliability of rotating machinery.

Vibration analysis remains a widely used diagnostic technique, however it remains complex because vibration signatures vary depending on the type of fault and the operating conditions of the machine.

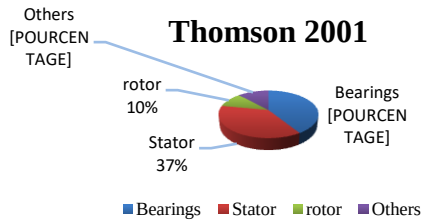

(a)

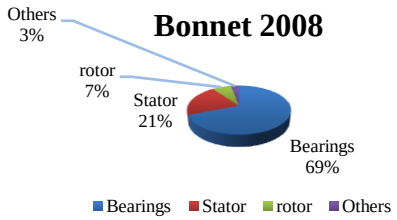

(b)

Figure 1. Statistics on defects in rotating machines (a) by Thomson in 2001 and (b) by Bonnet in 2008

Several research studies have explored the use of advanced techniques to improve fault detection in rotating machinery. Chan et al. (2025) proposed an approach based on the spectral characteristics of the vibration envelope to classify bearing defects. Other studies have integrated machine learning algorithms for failure prediction. These approaches are promising but require large volumes of data, complex models, and advanced expertise for implementation.

This article proposes a new, simple, and robust scalar indicator based on signal processing for industrial applications. This indicator highlights the differences in vibration behavior between a healthy bearing and bearings with specific defects (outer ring, inner ring, and ball cage). To better observe the discrimination of these defects compared to the healthy bearing, the indicator was tested on two datasets from different machines.

This article is structured as follows: After a brief review of the basic indicators associated with the newly developed indicator, the methodology used will be described. Next, the results obtained will be presented, and finally, their implications for industrial diagnostics will be discussed.

2. Materials and methods

2.1. Test benches and datasets

Two test benches served as the basis for the analyses:

2.1.1. Test bench 1

This test bench (*Figure 2*) is equipped with a 0.18 kW asynchronous motor operating at a rated speed of 1360 rpm, a variable speed drive, a load controller, a gear system, four bearings, a

FAT 20 ammeter/brake, and an 11 counts/rev tachometer. For vibration measurements specifically on the bearings, the gears were decoupled. Vibration sensors (accelerometers) are positioned on the bearings to measure the system's dynamic responses. The collected signals are recorded using the OROS analyzer-recorder. These signals include both healthy and faulty states at different frequencies (10 Hz, 20 Hz, 30 Hz, and 40 Hz). The signals are sampled at a frequency of 51200 Hz.

- *Instrumentation – Sensor:* The tachometer (Channel 1) of the device is a translational type with a resolution of 11 counts/rev, a sensitivity of 1 V/Hz, and a maximum bandwidth of 10 Hz. The accelerometers are also translational types, and their sensitivity and maximum bandwidth per measurement channel are as follows:
  - Channel 2: sensitivity 10.173 mV/m/s², maximum bandwidth 980 m/s²;
  - Channel 3: sensitivity 10.102 mV/m/s², maximum bandwidth 990 m/s²;
  - Channel 4: sensitivity 10.959 mV/m/s², maximum bandwidth 912 m/s²;
  - Channel 5: sensitivity 10.255 mV/m/s², maximum bandwidth 980 m/s²;
  - Channel 6: sensitivity 10.765 mV/m/s², maximum bandwidth 929 m/s².

The ammeter (brake) (Channel 7) is of the translation type, sensitivity 15 mV/A, its max band is 2.11 A.

The signals recorded on this bench reflect normal and degraded operating conditions at different frequencies, allowing for robust comparative analysis.

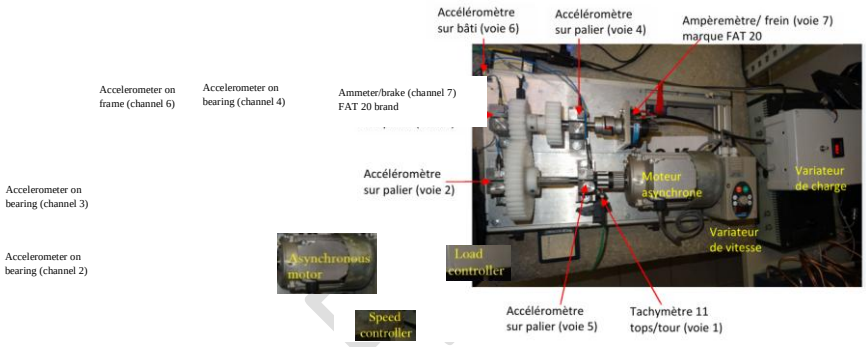

Figure 2. Test bench presented in the article « Evaluation des indicateurs de surveillance par analyse vibratoire : Application aux engrenages et r (& al. (2019)). The device includes a motor, a shaft, a gearbox, and a set of instrumented bearings.

2.1.2. Test bench2

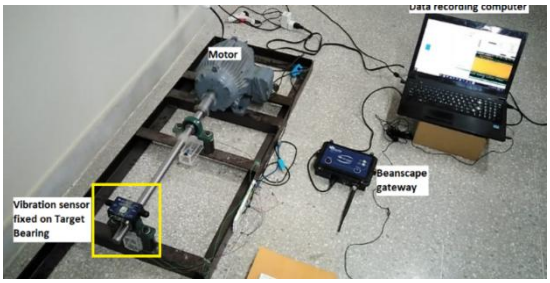

Figure 3. Test bench used by Aziz & al. (2023) for acquiring vibration signals from bearings. The mechanical device includes an electric motor, frame, bearings and shaft simulating different operating states: normal operation, inner ring defect and outer ring defect.

- *Experimental setup Motor:* A three-phase AC motor, 0.25 HP, operating at 1440 rpm (≈24 Hz), at a voltage of 440 volts, 50 Hz. Target bearings: The left bearing was replaced to represent three categories:
  - Normal bearing ;
  - Bearing with an inner ring defect;
  - Bearing with an outer ring defect.
- *Instrumentation - Sensor:* A Bean Device 2.4 GHz AX-3D wireless vibration sensor was used to record vibration data. This data was collected via Bean Gateway and stored on a PC. The sampling frequency was 1000 Hz. The recorded signals included both healthy and defective states, providing a complementary basis for comparison to that of bench 1.

The vibration signals collected from these two test benches (*Figures 1 and 2*) form the basis of the analyses conducted in this work. To evaluate the bearing fault discrimination capability, it is necessary to rely on relevant statistical indicators. Among the classic indicators, the Root Mean Square (RMS) and kurtosis are widely used to characterize the overall energy and the presence of impulse in the signals, respectively. However, each taken separately has limitations in the early detection of faults. It is in this context that a new indicator, denoted X, was developed by combining these two measurements to improve the robustness of the diagnosis. The methodology adopted is based on calculating these three indicators (RMS, kurtosis, and X) over time windows of 2, 4, 6, and 8 seconds, using MATLAB and Excel 2016, and then comparing their results to highlight the evolution and performance of the proposed indicator.

2.1.3. Bearings and their types of defects

A bearing is a mechanical component that sits between two parts of a machine, one rotating and the other stationary. Bearings have been used for a long time, but in a simplistic form. Today, bearings are taking on more sophisticated and varied forms, and their use in rotating machinery is becoming an absolute necessity (Oulmane, 2014).

A bearing consists of inner and outer rings, and a cage that separates the rolling elements (balls, rollers, needle, etc.) at specific distances (*Figure 4.a*). The cage's purpose is to keep the rolling elements inside the bearing and prevent them from leaving during operation, while still allowing rotation.

There are several types of bearings (Hotait, 2020): roller bearings (*figure 3.b*) supporting high radial and axial loads at low speeds; needle roller bearings (*figure 3.c*) having a high load capacity, especially at low speed, they are also suitable for high-speed applications; ball bearings (*figure 3.a*) used for low-load applications, and generally at the highest speeds.

The defects that can be encountered on bearings are as follows: spalling (*figure 4.d, e*), seizing, corrosion (which causes spalling) (*figure 4.b*), false Brinnel effect (*figure 4.c*), wear (*figure 4.a*), cage deformation (*figure 4.f*), etc... Most of these defects result in a loss of metal and cause repeated impacts of the balls on the bearing cage (Djebili, 2013).

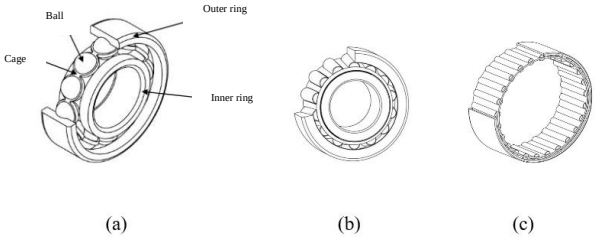

Figure 4. Bearing types (a) ball bearing (b) roller bearing (c) needle bearing (HOTAIT, 2020)

When a defect is present on a bearing element, the passage of the rolling element over the defect produces an impulsive force that causes the entire assembly to vibrate. The impulsive response oscillates at a natural frequency of the system, which quickly dissipates due to system damping. Each type of defect can be associated with a characteristic frequency, or defect frequency, which can be determined based on the bearing geometry, the number of balls, and the rotational speeds of the inner and outer rings. Different frequencies are generally obtained for defects on the outer ring, inner ring, cage, or on one of the rolling elements (Hotait, 2020).

Figure 5. (a) Wear of rolling elements (b) Corrosion of the outer ring (c) Friction of the rolling surface (Hamouche, 2022) (d) Defect on a ball (e) Spalling of the inner ring (e) Spalling of the outer ring (f) Deformation of the cage (HOTAIT, 2020)

2.2. Standard scalarindicators

2.2.1. Root Mean Square

Also called the RMS value, the Root Mean Square is the most commonly used scalar indicator for measuring the average energy of the signal. A bearing defect generally results in an increase in the RMS, linked to a higher vibration intensity.

$$RMS = \sqrt{\frac{\sum_{i=1}^{N}(x_i{}^2)}{N}} \quad \textit{Equation 1}$$

With N, the length of the vibrational signalx_i.

2.2.2. Kurtosis

Kurtosis is a measure of the degree to which a signal's amplitude distribution is flattened. It indicates the presence of peaks or pulses in the signal. Localized defects generate shocks that significantly increase this value.

Kurtosis is defined as the fourth-order moment of the amplitude distribution and is expressed by the equation below.

$$\boldsymbol{Kurtosis} = \frac{1}{N}\sum_{i=1}^{N}\frac{(x_i-\bar{x})^4}{\sigma^4} \quad \textit{Equation 2}$$

With $\bar{x}$, the mean and σ the standard deviation of the signal x_i.

2.2.3. Standard deviation

The standard deviation is the indicator that measures the variation of data values relative to the mean. A high value indicates that the data values are spread over a wide range, and conversely for a low value. The standard deviation can be used for the early detection of bearing defects. The equation below gives the expression for the standard deviation σ, where $\bar{x}$ is the mean of the data, and N is the length of the vibration signal x_i.

$$\sigma = \frac{1}{N}\sum_{i=1}^{N}\sqrt{x_i - \bar{x}} \quad \textit{Equation 3}$$

2.2.4. Proposedindicator

The developed indicator, denoted X, is a composite indicator. It combines measurements of the RMS value, Kurtosis, and a new parameter, the number of peaks above the RMS value ($N_{peaks\ >RMS}$), to enhance the ability to discriminate between healthy and defective states:

$$X = \frac{N_{peaks\ >RMS}\ .x_{RMS}}{Kurtosis} \quad \textit{Equation 4}$$

With $N_{pics\ >RMS}$ the number of peaks exceeding the RMS value (Example, see *figure 6*), RMS, the average energy of the signal, Kurtosis measuring the flattening of the distribution.

This composite indicator aims to simultaneously highlight the overall energy and the presence of pulses characteristic of defects.

Figure 6 below shows an example of the number of peaks above the RMS value extracted from a signal with an outer ring defect in a 0.003second time window. A total of 23 peaks can be observed, and the number of peaks above the RMS value is 3. The results for the three indicators RMS, Kurtosis, and X, in MATLAB, are 0.0001, 2.2983, and 0.0002, respectively.

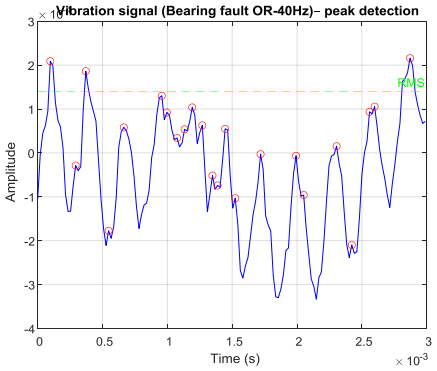

Figure 6. MATLAB result of $N_{peaks\ >RMS}$ for an outer ring defect on bench 1. Extraction over a window of 3.000000e-03 seconds.

2.3. TreatmentMethodology

- The signals were processed using MATLAB.
- Preprocessing consisted of normalizing and dividing the signals into time windows of 2, 4, 6, and 8 seconds.
- For each window, the RMS, Kurtosis, and X indicator values were calculated.
- A systematic comparison of the results was carried out in order to evaluate the ability of indicator X to discriminate defects in relation to classical indicators (RMS and Kurtosis), and also in relation to $N_{peaks\ >RMS}$.

2.4. Experimental Protocol

1. Extraction of vibration signals from the two databases.
2. Segmentation into time windows (2, 4, 6, 8 s).
3. Calculation of the RMS and Kurtosis values for each window.
4. Detection of peaks exceeding the RMS value.
5. Calculation of the composite indicator X.
6. Comparison of the results obtained with the RMS and Kurtosis indicators.

Thus, the entire experimental protocol, from signal collection on two separate test benches to the calculation of the RMS, Kurtosis, and new indicators X over different time windows, provides a solid basis for comparative analysis. The results presented in the following section will allow us to evaluate the relevance and performance of the indicator X in diagnosing bearing failures compared to conventional indicators.

3.1. Results RMS, Kurtosis and $N_{pics>RMS}$ on dataset 1

3.1.1. Evolution of the RMS value as a function of time windows and frequencies

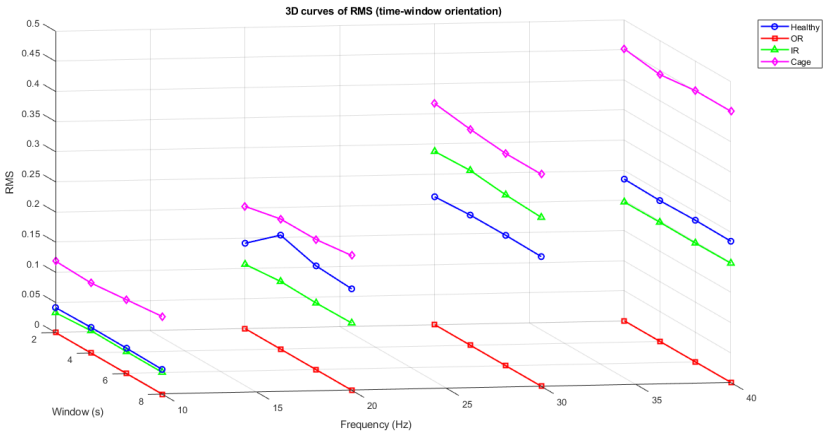

(a)

3. Résults

The analyses performed on the two datasets from the previously presented test benches allowed us to evaluate the performance of the new indicator X compared to the classic RMS and Kurtosis indicators, as well as the number of peaks exceeding RMS. Calculations were performed over time windows of 2, 4, 6, and 8 seconds to observe the evolution and stability of the values obtained according to the analysis duration. The results are organized to highlight:

- The ability of each indicator to discriminate between healthy and defective bearing conditions,
- The influence of the time window size on the sensitivity and stability of the indicators,
- The relevance of indicator X compared to reference measurements.

This section presents the results obtained for each dataset, followed by an overall comparison to identify trends and assess the added value of indicator X in bearing vibration diagnostics.

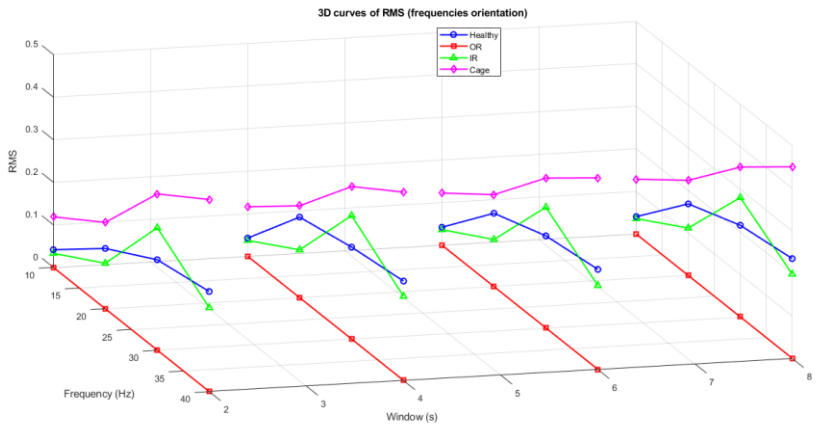

(b)

Figure 7. Evolution of the RMS value as a function of (a) time windows and (b) frequencies for dataset 1

3.1.2. *Evolution of Kurtosis as a function of time windows and frequencies*

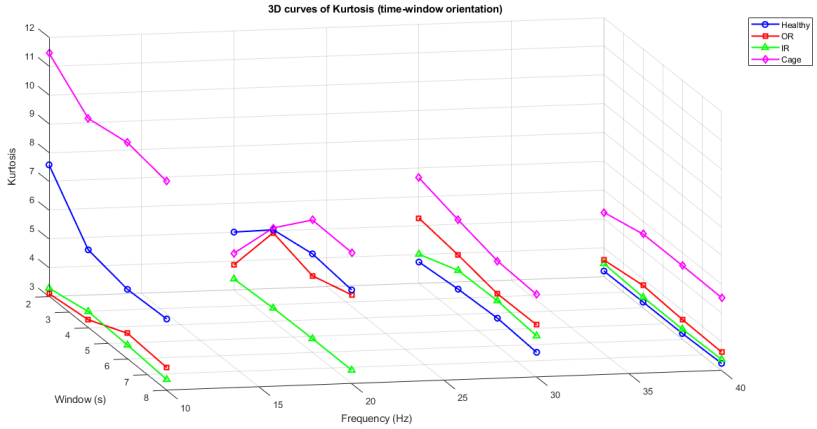

(a)

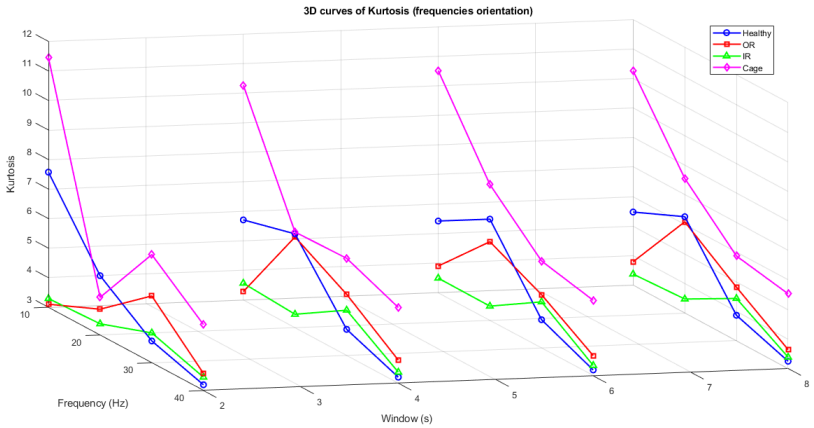

(b)

Figure 8. Evolution of Kurtosis as a function of (a) time windows and (b) frequencies for dataset 1

3.1.3. *Évolution du $N_{\text{pics}>RMS}$ en fonction des fenêtres temporelles et des fréquences*

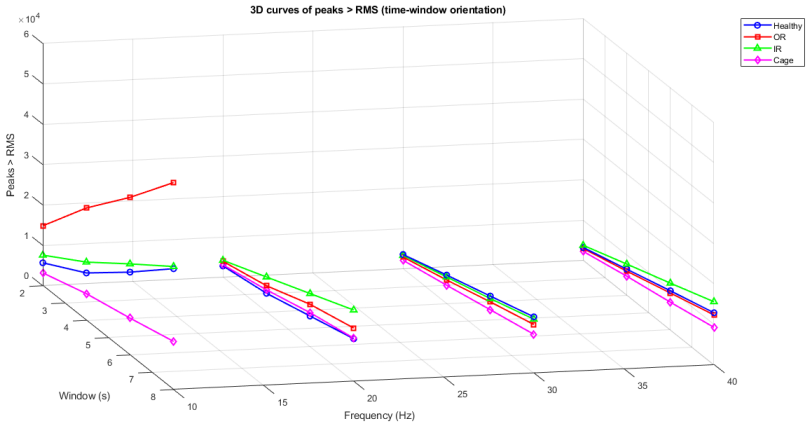

(a)

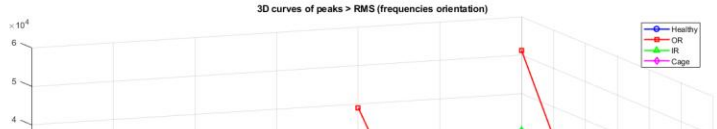

3.2. Results RMS, Kurtosis and $N_{pics>RMS}$ on dataset 2 as a function of time windows (frequencyof 24 Hz)

- ***Evolution of the RMS***

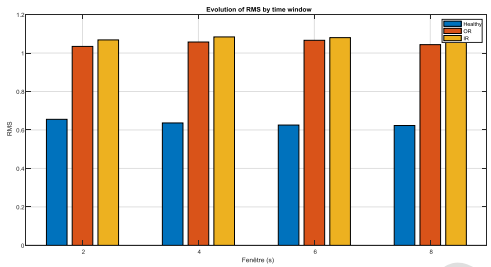

Figure 10. Evolution of RMS as a function of time windows for dataset 2

Legend: Clear separation between healthy state and defective states, but close values for BE and BI.

- ***Evolution of Kurtosis***

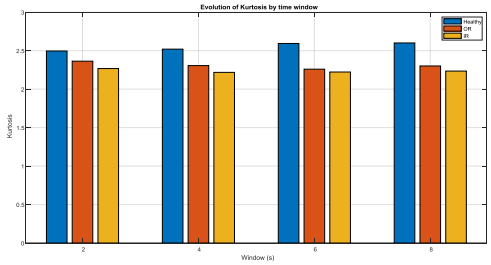

Figure 11. Evolution of Kurtosis as a function of windows for dataset 2

Legend: Homogeneous values around [2-2,6] for all states, confirming the low discriminatory capacity of Kurtosis.

- ***Evolution of the*** $N_{peaks} > RMS$

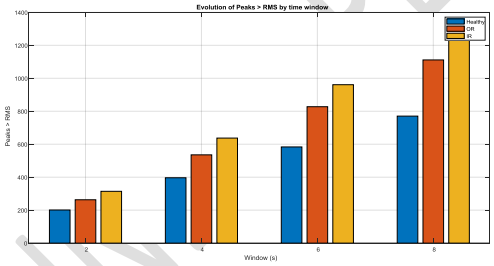

Figure 12. Number of peaks greater than RMS as a function of windows for dataset 2

Legend: Clear and hierarchical progression between states (healthy<OR<IR), confirming the robustness of this indicator.

3.3. Composite Indicator X

3.3.1. Result on dataset 1

- ***Evolution as a function of time windows***

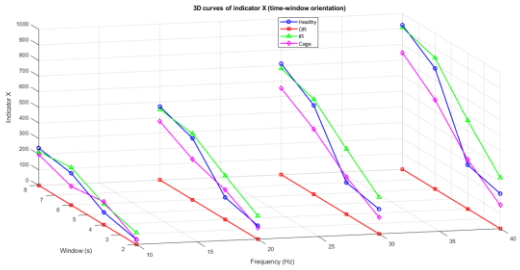

(a)

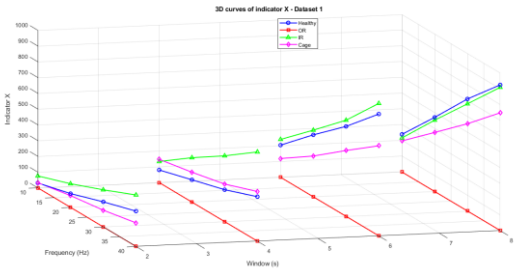

(b)

Figure 13. Evolution of indicator X as a function of (a) time windows and (b) frequencies (Dataset 1)

- ***Deviationsfrom a healthy state***

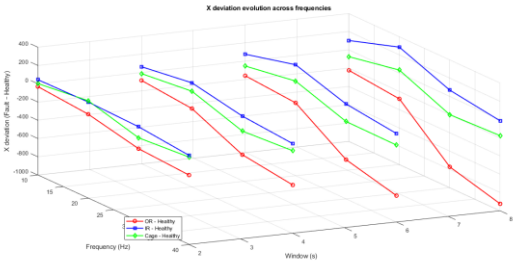

(a)

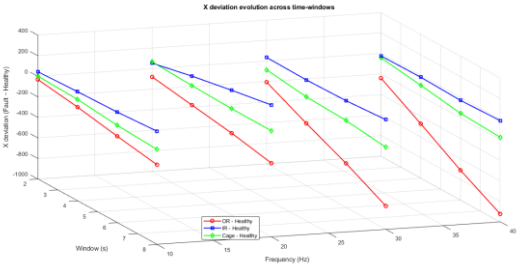

(b)

Figure 14. Deviation of indicator X between defective and healthy states for dataset 1: (a) frequency-based evolution, (b) time-window-based evolution

3.3.2. Result on dataset 2

- ***Evolution according to time windows (frequency of 24 Hz)***

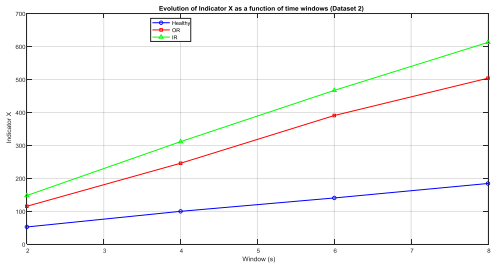

Figure 15. Evolution of indicator X as a function of time windows (dataset 2)

- ***Deviation fromhealthy***

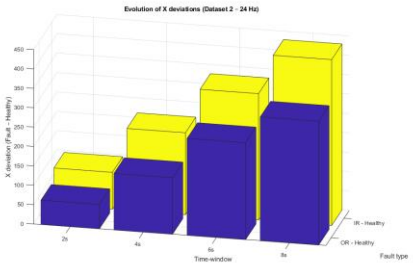

Figure 16. Difference between defective and healthy state of indicator X for dataset 2

4. Discussion

This section discusses the results obtained using classical indicators (RMS, Kurtosis), as well as $N_{peaks} > RMS$ and the composite indicator X, applied to the two datasets. The objective is to interpret the ability of these indicators to discriminate between healthy conditions and various bearing defects (outer ring, inner ring, cage), taking into account variations related to time windows and analysis frequencies. This discussion highlights the strengths and limitations of each indicator, as well as the added value of theindicator X from a robust vibration diagnostic perspective.

The results obtained highlight the limitations of classical indicators (RMS and Kurtosis), as well as of $N_{peaks} > RMS$ taken individually, in discriminating bearing states. Indeed, RMS, although it reflects the overall energy of the signal, sometimes exhibits very low or near-zero values for certain defects, which reduces its ability to clearly differentiate situations. Similarly, Kurtosis, sensitive to extreme distributions, varies significantly across time windows and does not always provide a clear separation between healthy and defective states. As for the number of peaks exceeding the RMS value, it reflects the presence of impulsive events but remains difficult to interpret on its own, as it can increase for both healthy and defective bearings. The composite indicator X, defined as($N_{peaks} > RMS \times RMS/Kurtosis$),overcomes these limitations by combining the three measurements in a balanced relationship. The results show that X amplifies the contrasts between the healthy state and defects, particularly for the inner ring where the values reach orders of magnitude significantly higher than those of the other configurations. Thus, X appears as a more robust and discriminating indicator, capable of highlighting structural differences between operating states, while reducing the ambiguities observed with conventional indicators.

4.1. Comparison of indicators on the two datasets

Comparison between the two datasets reveals an overall consistency in trends, but also notable differences related to experimental conditions.

4.1.1. RMS

In dataset 1, the RMS proved effective in distinguishing the sound state from inner ring (IR) and cage defects, but it failed to characterize the outer ring (OR) defect, whose values remained almost zero (*Figure 7*). In dataset 2, the RMS clearly separated the sound state from defective states, with higher values for OR and IR. However, the two defects had similar values, which limited the RMS's ability to differentiate between them (*Figure 10*). Comparison: The RMS is consistent in its ability to detect an increase in vibrational energy in the presence of defects, but it remains insufficient to discriminate between all types of defects, particularly OR.

4.1.2. Kurtosis

In dataset 1, Kurtosis showed higher values for healthy bearings and cage defects, but values close to statistical normality for OR and IR defects (*Figure 8*), limiting its discriminatory capacity. In dataset 2, Kurtosis values remained consistent (≈2.2–2.6) across all states, indicating low impulsivity and confirming its lack of robustness in separating defects (*Figure 11*). Comparison: In both datasets, Kurtosis proved to be of poor discriminatory power, except in certain specific cases (cage defects in dataset 1). Its consistency lies in its low sensitivity to OR and IR defects.

4.1.3. Number of peaks above RMS ($N_{peaks} > RMS$)

In dataset 1, the number of peaks above RMS showed a clear progression with the window and a clear distinction between states, particularly between healthy, OR defects, and IR defects (*Figure 9*). In dataset 2, this indicator confirmed its robustness, with a clear hierarchy: healthy <OR<IR (*Figure 12*). The values increase steadily with the window, reflecting an increasing density of vibration events. Comparison: in both datasets, the number of peaks above RMS is the most discriminating factor compared to conventional indicators (RMS and Kurtosis), offering a clear and consistent separation between states.

4.1.4. Consistency and relevance ofindicator X

Comparison of the two datasets (*Figures 13 and 16*) reveals overall consistency:

- RMS detects vibrational energy but remains limited for certain defects.
- Kurtosis is not very discriminating, except in specific cases.
- $N_{peaks} > RMS$is the most robust and consistent, allowing for clear prioritization.

This complementarity fully justifies the development of the X indicator, which combines RMS, Kurtosis, and $N_{peaks} > RMS$. In both datasets, X overcomes individual limitations and provides a clear separation between rolling states. Its relevance is reinforced by the consistency of the observations: regardless of the experimental condition (various frequencies or constant frequency), X remains reliable and discriminating.

4.1.5. Difference between healthy and faulty states for X indicator

Analysis of the differences in indicator X between the healthy and defective states reveals contrasting behaviors depending on the dataset and experimental conditions.

In dataset 1, the differences in X (*Figure 15*) show strong variability depending on frequencies and time windows.

- The Outer Ring (OR) defect consistently exhibits very low X values, generating significant negative deviations compared to the healthy bearing. This reflects the difficulty the indicator has in capturing this type of defect, likely due to its low vibrational energy.
- The Inner Ring (IR) defect is distinguished by positive deviations that increase with the window size and frequency. These deviations reach high values, confirming X's ability to effectively discriminate this defect.
- The cage defect shows intermediate deviations: sometimes positive, sometimes close to the healthy value, but overall significant. This reflects a particular vibrational impulsivity, which is well captured by the X indicator.

In dataset 2 (Frequency of 24 Hz), the deviations of X (*Figure 17*) are more stable and consistent.

- Defects OR and IR exhibit X values significantly higher than those of the healthy bearing, generating positive and increasing deviations with the window size.
- Unlike dataset 1, the OR defect is clearly distinguished here, with significant deviations even at the 2second window.
- The IR defect confirms its tendency to produce the highest deviations, reflecting a robust vibration signature that is easily identifiable by X.

4.1.6. Comparison between the two datasets

Comparing the two datasets highlights the importance of experimental conditions.

- In set 1, X performs well for IR and cage defects, but is limited for OR defects.
- n set 2, X effectively discriminates all defects, with positive and increasing differences.
- Overall, X indicator appears to be a robust solution, but its sensitivity can be influenced by the nature of the signal and the measurement conditions.

4.2. Implications for predictive maintenance

These results confirm that indicator X represents a significant improvement compared to classic indicators (RMS, Kurtosis).

- It allows for clear discrimination of defects in most cases.
- It offers better consistency when measurement conditions are stable (set 2).
- It can be used as a primary indicator in a vibration diagnostic strategy, while taking into account its limitations for certain defects under unstable measurement conditions.

In practice, using the X indicator as an alert threshold would allow for anticipating failures, planning maintenance interventions, and optimizing equipment lifespan. It thus represents a significant advancement for monitoring rotating machinery and reducing costs associated with unplanned downtime.

Comparing conventional indicators with the X indicator shows that the X indicator represents a significant advancement for bearing vibration diagnostics. Its ability to combine energy, impulsivity, and peak density makes it a robust and discriminating tool, particularly well-suited to predictive maintenance applications.

4.3. Conclusion and perspectives

The analyses conducted on both datasets highlight the consistency and complementarity of the results. In the first dataset, performed at different frequencies (10, 20, 30, 40 Hz), the X indicator proved to be the most discriminating, surpassing RMS and Kurtosis in detecting bearing defects. In the second dataset, measured at a constant frequency of 24 Hz, or 1440 rpm, RMS demonstrated a better ability to distinguish between healthy and defective states, but the X indicator confirmed its superiority by providing a clear and hierarchical separation between the different defects.

These observations highlight the robustness of the X indicator, capable of providing reliable diagnoses in a variety of experimental contexts. Its simplicity of calculation, its sensitivity to defects, and its ability to integrate multiple dimensions of the vibration signal make it a particularly suitable tool for condition-based and predictive maintenance.

However, certain limitations must be considered, notably the need to validate the indicator on larger databases and in real-world industrial environments. These validations will confirm its robustness to external disturbances and allow for comparison of its performance with other leading indicators.

Looking ahead, the X indicator could be integrated into real-time monitoring systems, coupled with artificial intelligence algorithms to improve automatic fault classification, and extended to other types of rotating machinery, particularly under conditions that take into account variations in speed and/or load. These developments pave the way for proactive maintenance, capable of anticipating failures, reducing unplanned downtime, and optimizing equipment lifespan.

Thus, the results obtained show that the composite indicator X offers superior discriminatory power compared to conventional metrics. Its simplicity of calculation and experimental relevance make it a promising tool for predictive maintenance strategies, particularly in industrial environments where bearing reliability is critical.

References

1. Taleb Mounia (2018), "Surveillance, détection et diagnostic des défaillances dans une cimenterie en utilisant l'analyse fonctionnelle." [Monitoring, detection and diagnosis of failures in a cement plant using functional analysis.], thesis, Université du 20 Août 1955 Skikda.
2. Hassane Hotait(2020), " Contribution au processus de surveillance intelligente des machines tournantes : cas des roulements à billes."[Contribution to the intelligent monitoring process of rotating machines: case of ball bearings.],thesis, Université de Reims Champagne-Ardenne.
3. Sanaa Kerroumi(2016), "Extraction des paramètres et classification dynamique dans le cadre de la détection et du suivi de défaut de roulements" [Parameter extraction and dynamic classification in the context of bearingfaultdetection and monitoring], thesis, université de Reims Champagne-Ardenne.

4. Oianquian Zhang, Caiyun Hao, Chan Xu (2025), " Intelligent fault diagnosis of rotating machinery based on improved hybrid dilated convolution network for unbalanced samples", article.

5. ABDELHAKIM BOUKAR& NACER HAMZAOUI (2019), "Evaluation des indicateurs de surveillance par analysevibratoire : Application aux engrenages et roulement" [Evaluation of monitoring indicators by vibration analysis: Application to gears and bearings], article, INSTA

6. AZIZ, S., KHAN, M. U., FARAZ, M., & MONTES, G. A. (2023). Intelligent bearing faults diagnosis featuring automated relative energy-based empirical mode decomposition and novel cepstral autoregressive features. Measurement, 216, 112871.

7. Khalil HAMOUCHE, "Surveillance multi dimensionnelle des machines tournantes par classification dynamique dans un but de maintenance conditionnelle" [Multidimensional monitoring of rotating machines by dynamic classification for the purpose of condition-based maintenance], Thesis, Université de Reims Champagne-Ardenne et Université de Sétif1 Ferhat ABBAS, 2022.

8. OULMANE, A. (2014). "Surveillance et diagnostic des défauts des machines tournantes dans le domaine temps-fréquences utilisant les réseaux de neurones et la logique floue" [Monitoring and diagnosis of rotatingmachineryfaults in the time-frequencydomainusing neural networks and fuzzylogic],Thesis, École Polytechnique de Montréal. PolyPublie. https://publications.polymtl.ca/1469/.